Chapter 3

Numerical Method

3.1 Introduction

This chapter discusses the numerical approach used to discretize and solve the system of non-linear partial differential equations developed in the previous chapter. The finite volume formulation is introduced, and the methods used to evaluate the inviscid and viscous flux terms are presented. Finally, the basic starting equation used to advance the solution forward in time is derived.

3.2 Finite Volume Formulation

This section outlines the discretization of the equation set using the finite volume technique. The conservation equations presented in Chapter 2 must first be converted to a general curvilinear coordinate system, using the transformation

$$\begin{aligned} \frac{\partial}{\partial \xi} &= \frac{\partial}{\partial x}\frac{\partial x}{\partial \xi} + \frac{\partial}{\partial y}\frac{\partial y}{\partial \xi}, \\ \frac{\partial}{\partial \eta} &= \frac{\partial}{\partial x}\frac{\partial x}{\partial \eta} + \frac{\partial}{\partial y}\frac{\partial y}{\partial \eta}, \end{aligned} \tag{3.1}$$

where ξ is defined as the body-tangential and η the body-normal direction. After this transformation, the governing equations can be written in conservation form as

$$\frac{\partial U}{\partial t} + \frac{\partial \tilde{F}}{\partial \xi} + \frac{\partial \tilde{G}}{\partial \eta} = W, \tag{3.2}$$

where U is the vector of conserved quantities, $\tilde{F}$ and $\tilde{G}$ are the flux vectors in the ξ and η directions, and W is the vector of source terms. In this curvilinear coordinate system $\tilde{F}$ and $\tilde{G}$ are functionally equivalent. Details of this transformation can be

found in Candler (1988) or Hirsch (1991). The resulting flux vectors can be split into convective (inviscid) and viscous parts

$$\tilde{F} = F + F_v, \qquad \tilde{G} = G + G_v. \tag{3.3}$$

Under the approximations listed in the previous chapter, the conserved quantity, flux, and source term vectors for a two-dimensional thermochemical nonequilibrium air flow can be written as

$$U = \begin{pmatrix} \rho_1 \\ \rho_2 \\ \vdots \\ \rho_s \\ \rho u \\ \rho v \\ E_v \\ E \end{pmatrix}, \quad F = G = \begin{pmatrix} \rho_1 u' \\ \rho_2 u' \\ \vdots \\ \rho_s u' \\ \rho u u' + p s_x \\ \rho v u' + p s_y \\ E_v u' \\ (E+p)u' \end{pmatrix}$$

$$F_v = G_v = -\begin{pmatrix} \rho \mathcal{D}(\frac{\partial c_1}{\partial x} s_x + \frac{\partial c_1}{\partial y} s_y) \\ \rho \mathcal{D}(\frac{\partial c_2}{\partial x} s_x + \frac{\partial c_2}{\partial y} s_y) \\ \vdots \\ \rho \mathcal{D}(\frac{\partial c_s}{\partial x} s_x + \frac{\partial c_s}{\partial y} s_y) \\ \tau_{xx} s_x + \tau_{xy} s_y \\ \tau_{xy} s_x + \tau_{yy} s_y \\ (\rho \sum_{nd} e_{vs} \mathcal{D} \frac{\partial c_s}{\partial x} + q_{vx}) s_x + \\ (\rho \sum_{nd} e_{vs} \mathcal{D} \frac{\partial c_s}{\partial y} + q_{vy}) s_y \\ (\tau_{xx} u + \tau_{xy} v + q_x + q_{vx} + \rho \sum_{ns} h_s \mathcal{D} \frac{\partial c_s}{\partial x}) s_x + \\ (\tau_{xy} u + \tau_{yy} v + q_y + q_{vy} + \rho \sum_{ns} h_s \mathcal{D} \frac{\partial c_s}{\partial y}) s_y \end{pmatrix}, \quad W = \begin{pmatrix} w_1 \\ w_2 \\ \vdots \\ w_s \\ 0 \\ 0 \\ w_v \\ 0 \end{pmatrix}, \tag{3.4}$$

where s_x, s_y are the local direction cosines of the curvilinear coordinate system, and u' is the normal velocity component, defined as

$$u' = u s_x + v s_y. \tag{3.5}$$

A similar result is obtained for perfect gas flows. In the finite volume formulation we solve Eqs. (3.2) by integrating them over an arbitrary control volume V. Green's

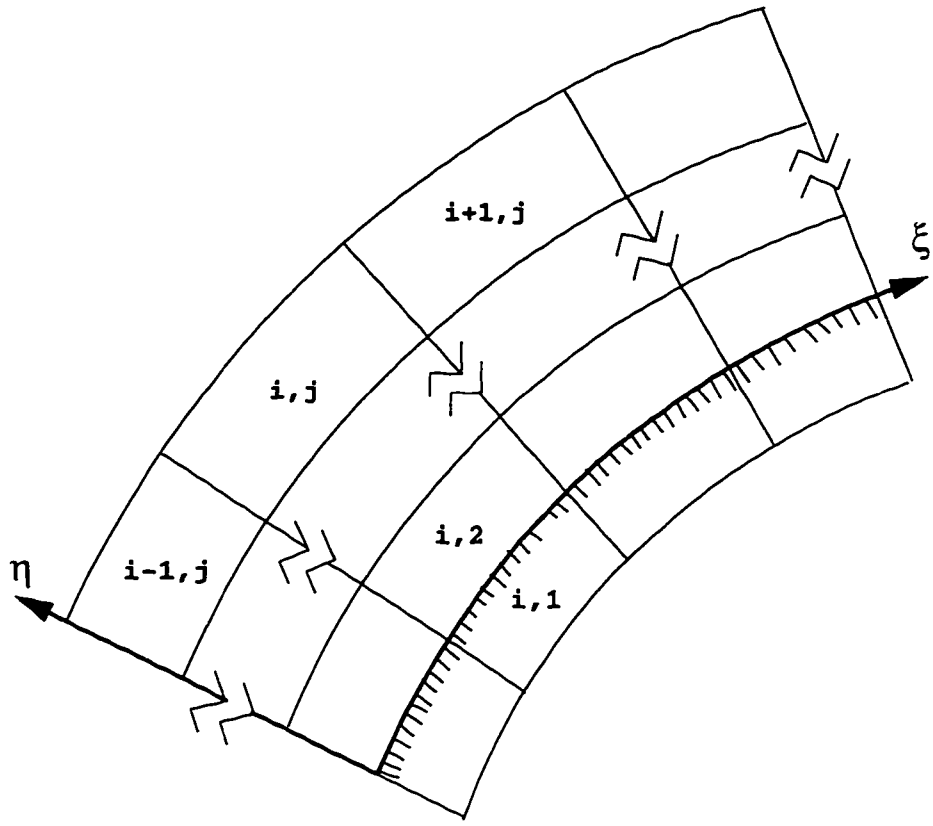

Fig. 3.1 Schematic diagram of a typical two-dimensional finite volume grid. A solid wall is located between $j=1$ and $j=2$.

Theorem is then used to convert the volume integral containing the flux vectors into a surface integral, resulting in

$$\frac{\partial U}{\partial t} + \frac{1}{V}\int_s \tilde{F}\cdot dS = W, \tag{3.6}$$

where V is the volume, $\tilde{F}\cdot dS$ is the total flux through the surface S, and U and W are assumed constant within the control volume. Now, we discretize the problem by dividing the computational space into a series of volume elements. This is typically done by laying out a regular curvilinear mesh over the solution domain, resulting in a structured grid on which, for two-dimensional problems, each computational cell is a four-sided polygon. A sample portion of such a structured grid is shown in Fig. (3.1). In the figure, the grid directions are defined such that i increases in the ξ-direction and j increases in the η-direction. In the finite volume method flow variables are stored at the cell centers, rather than the nodes. Data at the

cell faces is then found by some sort of averaging procedure. Because of this, an extra line of cells, called "dummy" cells, is usually included along the boundaries of the grid. These dummy cells are used to store the necessary boundary conditions for the problem. In Fig. (3.1) there is a solid wall boundary at $j = 3/2$, and the $j = 1$ cells are the dummy cells located inside the solid wall. The interior of the computational domain then begins at $j=2$.

For a 2-D volume element i, j we can represent the time rate of change of U as the sum of the fluxes through the four cell faces and the source of U within the volume, as in

$$\frac{\partial U_{i,j}}{\partial t} = -\frac{1}{V_{i,j}}(\tilde{F}_{i+1/2,j}S_{i+1/2,j} - \tilde{F}_{i-1/2,j}S_{i-1/2,j} + \tilde{G}_{i,j+1/2}S_{i,j+1/2} - \tilde{G}_{i,j-1/2}S_{i,j-1/2}) + W_{i,j}. \tag{3.7}$$

The $\pm 1/2$ indices on the flux and surface area terms indicate that they should be evaluated at the appropriate cell face. This expression represents the discretized form of the conservation equations. An analogous set of expressions can easily be derived for three-dimensional flow, where in that case the volume elements are six-sided polyhedra.

3.3 Evaluation of the Fluxes

There are many different methods in the literature for evaluating the right-hand side of Eq. (3.7). The solution is complicated by the fact that the inviscid fluxes are hyperbolic, while the viscous fluxes are elliptic in nature. For this reason the viscous fluxes are typically evaluated using simple central differencing [Hirsch (1991)], while a more sophisticated approach is required for the evaluation of the inviscid flux. Most modern solution methods for the inviscid flux terms take advantage of the fact that there are definable characteristic directions in the flow, and thus the required derivatives should be taken following these characteristic directions. This is commonly referred to as upwind biasing. One such method that has been widely used due to its simplicity and robustness is Steger-Warming (1981)

flux-vector splitting. A brief derivation of this method is included here not only because it is the primary method used in this research, but also because some of the concepts introduced will be useful in the following chapters when the implicit time advancement algorithms developed in this work are presented.

3.3.1 Inviscid Fluxes

First, we focus on the inviscid problem. We will return to the evaluation of the viscous fluxes in the next section. The first step in the evaluation of the inviscid fluxes is to use the fact that they are homogeneous in the vector of conserved quantities U, such that

$$F(\lambda U) = \lambda F(U), \tag{3.8}$$

where λ is any scalar. This can easily be shown from the governing equations developed in Chapter 2. From this it is possible to linearize the flux vector, using

$$\begin{aligned} F &= \left(\frac{\partial F}{\partial U}\right)U = AU, \\ G &= \left(\frac{\partial G}{\partial U}\right)U = BU, \end{aligned} \tag{3.9}$$

where A and B are the inviscid flux Jacobian matrices in the ξ and η directions, respectively.

We then split the fluxes into positively-moving and negatively-moving components using an upwind biasing scheme. In the Steger-Warming formulation the fluxes are split according to the sign of the eigenvalues of the Jacobians. Therefore, we must calculate the eigenvalues and eigenvectors of A. In order to do this we first break the Jacobian matrices into components that will be easier to work with

$$A = \frac{\partial U}{\partial V}\frac{\partial V}{\partial U}\frac{\partial F}{\partial V}\frac{\partial V}{\partial U}, \tag{3.10}$$

where V is a vector of primitive variables, introduced purely as a convenience to simplify the computation of A. The choice of V is not unique, but for the inviscid fluxes it is convenient to use

$$V = \left(\rho_1, \rho_2, \ldots, \rho_s, u, v, e_v, p\right)', \tag{3.11}$$

where e_v is the total vibrational energy per unit mass. $\frac{\partial U}{\partial V}$ and $\frac{\partial V}{\partial U}$ are the transformation matrices between primitive and conserved variables, and are denoted by S^{-1} and S respectively. This transformation is made because the remaining matrix $\frac{\partial V}{\partial U}\frac{\partial F}{\partial V}$ is much easier to diagonalize than A. The diagonalization itself is now straightforward, using basic linear algebra

$$\frac{\partial V}{\partial U}\frac{\partial F}{\partial V} = R^{-1}\Lambda R, \tag{3.12}$$

where Λ is the diagonal matrix of eigenvalues of the system, and R^{-1} and R are the left and right eigenvector matrices. These required matrices are given in the Appendix for a perfect gas flow, and the results are easily extended to reacting flows as well.

The flux vector can now be split into positively-moving and negatively-moving components, based on the sign of the eigenvalues. The split fluxes F_+ and F_- are defined by

$$\begin{aligned} F_+ &= S^{-1}R^{-1}\Lambda_+ RSU = A_+ U, \\ F_- &= S^{-1}R^{-1}\Lambda_- RSU = A_- U, \end{aligned} \tag{3.13}$$

where Λ_+ and Λ_- are the split eigenvalue matrices consisting of only the positive and negative eigenvalues, respectively. A_+ and A_- are the corresponding positive and negative Jacobians. The total inviscid flux vector through each cell face can then be expressed as the sum of positively and negatively moving components, as in

$$\begin{aligned} F_{i+\frac{1}{2},j} &= F_{+i+\frac{1}{2},j} + F_{-i+\frac{1}{2},j}, \\ G_{i,j+\frac{1}{2}} &= G_{+i,j+\frac{1}{2}} + G_{-i,j+\frac{1}{2}}. \end{aligned} \tag{3.14}$$

The split fluxes at each cell face are calculated using

$$\begin{aligned} F_{+\,i+\frac{1}{2},j} &= A_{+\,i,j}U_{i,j}, \\ F_{-\,i+\frac{1}{2},j} &= A_{-\,i+1,j}U_{i+1,j}, \end{aligned} \tag{3.15}$$

where A and U are evaluated based on data at the upwind cell center. However, in practice we usually evaluate the Jacobian matrices at the cell faces rather than the

upwind cell centers, as in

$$\begin{aligned} F_{+i+\frac{1}{2},j} &= A_{+i+\frac{1}{2},j} U_{i,j}, \\ F_{-i+\frac{1}{2},j} &= A_{-i+\frac{1}{2},j} U_{i+1,j}. \end{aligned} \tag{3.16}$$

This modification of the original Steger-Warming method was proposed by MacCormack and Candler (1989), and has been shown to greatly reduce the amount of numerical dissipation in the method. While this modified approach works well in regions of weak gradients, additional dissipation is required to capture strong gradients, such as shock waves. Therefore, a hybrid approach is usually used, in which the Jacobian matrices are evaluated using a pressure weighted average of quantities in the adjacent cells. In this way the method will smoothly switch from modified to true Steger-Warming in regions of high pressure gradients. If we then substitute the split fluxes into Eq. (3.7), we get the standard upwind finite volume representation of the inviscid problem

$$\begin{aligned} \frac{\partial U_{i,j}}{\partial t} = -\frac{1}{V_{i,j}} \Big\{ & \left(A_{+i+\frac{1}{2},j} S_{i+\frac{1}{2},j} U_{i,j} - A_{+i-\frac{1}{2},j} S_{i-\frac{1}{2},j} U_{i-1,j} \right) \\ & - \left(A_{-i-\frac{1}{2},j} S_{i-\frac{1}{2},j} U_{i,j} - A_{-i+\frac{1}{2},j} S_{i+\frac{1}{2},j} U_{i+1,j} \right) \\ & + \left(B_{+i,j+\frac{1}{2}} S_{i,j+\frac{1}{2}} U_{i,j} - B_{+i,j-\frac{1}{2}} S_{i,j-\frac{1}{2}} U_{i,j-1} \right) \\ & - \left(B_{-i,j-\frac{1}{2}} S_{i,j-\frac{1}{2}} U_{i,j} - B_{-i,j+\frac{1}{2}} S_{i,j+\frac{1}{2}} U_{i,j+1} \right) \Big\} + W_{i,j}. \end{aligned} \tag{3.17}$$

The Steger-Warming method as formulated has only first-order spatial accuracy, although it is possible to achieve second-order accuracy in regions of weak gradients with a minor modification. While this is sufficient for many problems, a higher order accurate scheme may be preferred for certain applications. In general schemes with higher order spatial accuracy are less dissipative, and can produce a more resolved solution on a given computational mesh. Therefore, if it is desired to resolve flow features that can be easily smeared by the numerical dissipation present in the scheme, such as weak shear layers, a high order accurate scheme may be required. Unfortunately, while there are a great many high order accurate schemes available, most suffer from numerical difficulties when used to simulate flows in

which strong shocks are present. In certain cases these schemes require so many extra time steps to achieve a steady-state solution that an equivalent solution can be obtained in less time on a more resolved grid using a first-order method [Olejniczak *et al.* (1996a)]. Several second-order accurate methods have been used in this research when required, including a Harten-Yee (1989) upwind total variation diminishing (TVD) method, and a symmetric TVD method proposed by Gnoffo (1990).

3.3.2 Viscous Fluxes

As discussed earlier, the elliptic nature of the viscous fluxes makes them much simpler to compute than the inviscid component. The viscous flux vector outlined in Eq. (3.4) is simply evaluated at the required cell faces using central differencing, resulting in a flux through each face of the form

$$F_{v\,i+\frac{1}{2},j} S_{i+\frac{1}{2},j}. \tag{3.18}$$

The contribution of the viscous fluxes is then summed through each of the four cell faces (six in three-dimensional flow) and added to Eq. (3.17) above. A detailed discussion of the formulation of these fluxes and the calculation of the required derivatives can be found in Hirsch (1991).

3.4 Time Advancement

Up to this point we have made no effort to evaluate the time derivative on the left-hand side of Eq. (3.17). This term must also be discretized in some manner in order to time-march the solution toward a steady-state answer. The simplest form of time advancement that is used is first-order forward Euler differencing, in which the time derivative is expressed

$$\frac{\partial U_{i,j}}{\partial t} \simeq \frac{U_{i,j}^{n+1} - U_{i,j}^{n}}{\Delta t} = \frac{\Delta U_{i,j}^{n}}{\Delta t}. \tag{3.19}$$

In this expression, the superscript denotes the time level of the solution, which is advanced from the current time n to the next level $n+1$. Expressions for the

time derivative may of course be obtained to any order of accuracy, using Runge-Kutta or other differencing methods. The resulting expression is then substituted directly into Eq. (3.17) and the solution is marched forward in time by discrete time steps. For the Euler method detailed above, the explicit formulation of the inviscid problem becomes

$$\begin{aligned}\Delta U^n_{i,j} = -\frac{\Delta t}{V_{i,j}}\Big\{&\left(A_{+i+\frac{1}{2},j}S_{i+\frac{1}{2},j}U_{i,j} - A_{+i-\frac{1}{2},j}S_{i-\frac{1}{2},j}U_{i-1,j}\right)\\ &-\left(A_{-i-\frac{1}{2},j}S_{i-\frac{1}{2},j}U_{i,j} - A_{-i+\frac{1}{2},j}S_{i+\frac{1}{2},j}U_{i+1,j}\right)\\ &+\left(B_{+i,j+\frac{1}{2}}S_{i,j+\frac{1}{2}}U_{i,j} - B_{+i,j-\frac{1}{2}}S_{i,j-\frac{1}{2}}U_{i,j-1}\right)\\ &-\left(B_{-i,j-\frac{1}{2}}S_{i,j-\frac{1}{2}}U_{i,j} - B_{-i,j+\frac{1}{2}}S_{i,j+\frac{1}{2}}U_{i,j+1}\right)\Big\}^n + \Delta t W^n_{i,j}.\end{aligned} \tag{3.20}$$

where $\Delta U^n_{i,j}$ is the explicit residual, or change of solution vector. The solution is then updated to the next time level using

$$U^{n+1}_{i,j} = U^n_{i,j} + \Delta U^n_{i,j}. \tag{3.21}$$

This is called an explicit method because the change of solution vector on the left-hand side of Eq. (3.20) can be obtained explicitly by evaluating the right-hand side at time level n. In other words, the solution at any point at the new time level $n+1$ is not dependent on the solution of other points at time level $n+1$.

While explicit time advancement methods can be useful for the solution of unsteady problems, where time accuracy is important, they are not effective for the simulation of most steady-state flows. This is because the numerical stability of the method imposes a maximum stable time step, which will in general be much smaller than the time required to reach a steady-state solution. This time step is based on the length of time it takes information to traverse a computational cell, and therefore will be dependent not only on the fluid dynamics, but also on the mesh spacing. For the one-dimensional Euler equations, the maximum stable time step can be shown to be

$$\Delta t_{max} = \frac{\Delta x}{|u| + a}.$$

Unfortunately, no proof of stability exists for the two- or three-dimensional case, although a similar definition is typically used. In practice, some fraction of Δt_{max} is typically chosen, and the actual time step is given by

$$\Delta t = CFL\,\Delta t_{max},$$

where CFL is the Courant-Fredereichs-Lewy number. Therefore, if it is desired to use an explicit method to reach a steady-state solution, a large number of iterations (time steps) will be required, especially on a highly resolved grid.

The use of an implicit method can allow much larger time steps to be taken. Therefore, a dramatic time-savings is possible in the solution of steady-state problems with the use of such implicit methods. In a true implicit method, the solution at any point in the grid is dependent on the solution of all other points at the new time level $n+1$. Therefore, in order to implement an implicit time advancement method it is necessary to evaluate the fluxes at time level $n+1$. The fully implicit upwind formulation of the inviscid problem can be expressed as

$$\begin{aligned}\delta U^n_{i,j} = -\frac{\Delta t}{V_{i,j}}(&F_{+i+1/2,j}S_{i+1/2,j} - F_{+i-1/2,j}S_{i-1/2,j} + \\ &F_{-i+1/2,j}S_{i+1/2,j} - F_{-i-1/2,j}S_{i-1/2,j} + \\ &G_{+i,j+1/2}S_{i,j+1/2} - G_{+i,j-1/2}S_{i,j-1/2} + \\ &G_{-i,j+1/2}S_{i,j+1/2} - G_{-i,j-1/2}S_{i,j-1/2})^{n+1} + \Delta t\, W^{n+1}_{i,j},\end{aligned} \tag{3.22}$$

where $\delta U^n_{i,j}$ is the change in the solution between time levels n and $n+1$. Now the fluxes and the source term vector are linearized in time and space

$$\begin{aligned}F^{n+1}_{i,j} &= F^n_{i,j} + \Big(\frac{\partial F}{\partial U}\Big)^n_{i,j}(U^{n+1}_{i,j} - U^n_{i,j}) + \mathcal{O}(\Delta t^2) \\ &\simeq F^n_{i,j} + A^n_{i,j}\delta U^n_{i,j} \\ W^{n+1}_{i,j} &\simeq W^n_{i,j} + C^n_{i,j}\delta U^n_{i,j},\end{aligned} \tag{3.23}$$

where $C^n_{i,j}$ is the source term Jacobian. This linearization is applied to the split fluxes in the same upwind biased manner described above, and the fully implicit

upwind formulation of the problem can be expressed by substituting the linearized fluxes into Eq. (3.22)

$$\begin{aligned}\delta U^n_{i,j} + \frac{\Delta t}{V_{i,j}}\Big\{ &\left(A_{+i+\frac{1}{2},j} S_{i+\frac{1}{2},j} \delta U_{i,j} - A_{+i-\frac{1}{2},j} S_{i-\frac{1}{2},j} \delta U_{i-1,j}\right) \\ &-\left(A_{-i-\frac{1}{2},j} S_{i-\frac{1}{2},j} \delta U_{i,j} - A_{-i+\frac{1}{2},j} S_{i+\frac{1}{2},j} \delta U_{i+1,j}\right) \\ &+\left(B_{+i,j+\frac{1}{2}} S_{i,j+\frac{1}{2}} \delta U_{i,j} - B_{+i,j-\frac{1}{2}} S_{i,j-\frac{1}{2}} \delta U_{i,j-1}\right) \\ &-\left(B_{-i,j-\frac{1}{2}} S_{i,j-\frac{1}{2}} \delta U_{i,j} - B_{-i,j+\frac{1}{2}} S_{i,j+\frac{1}{2}} \delta U_{i,j+1}\right)\Big\}^n \\ &+\Delta t\, C^n_{i,j} \delta U^n_{i,j} = \Delta U^n_{i,j},\end{aligned} \tag{3.24}$$

For the solution of viscous flows, Eq. (3.24) must be modified to include the contribution of the appropriate implicit viscous terms. Following the methods of Tysinger and Caughey (1991), or Gnoffo (1990), we can linearize the viscous flux vectors F_v and G_v, assuming that the transport coefficients are locally constant, to obtain

$$F^{n+1}_v \simeq F^n_v + \frac{\partial}{\partial \xi}(L\delta U)^n, \quad G^{n+1}_v \simeq G^n_v + \frac{\partial}{\partial \eta}(N\delta U)^n, \tag{3.25}$$

where the viscous Jacobians L and N are evaluated in such a way that they are functions of the vector of conserved quantities U, and not the derivatives of U. Note that in general F_v will be a function of U, U_ξ, and U_η, and thus the viscous Jacobians in Eq. (3.25) are only approximate. However, these expressions have been used effectively in a variety of algorithms. The viscous Jacobians are reproduced in the Appendix for perfect gas flows, but again the extension to chemically reacting flows is straightforward. With these definitions Eq. (3.24) will be unchanged if we simply replace the Euler Jacobians A and B with $\tilde{A}$ and $\tilde{B}$, where

$$\begin{aligned}\tilde{A}_+ &= A_+ - L, \qquad \tilde{A}_- = A_- + L, \\ \tilde{B}_+ &= B_+ - N, \qquad \tilde{B}_- = B_- + N.\end{aligned} \tag{3.26}$$

In principle, Eq. (3.24) can be solved directly for $\delta U^n_{i,j}$. However, with all of the off-diagonal terms on the left-hand side of the equation, the entire flowfield is fully coupled. Therefore, the entire left-hand side of the equation must be solved in

a fully implicit fashion, using a matrix inversion. A direct solution of this equation would thus require the formation and inversion of a large block banded matrix. which is too numerically intensive for practical problems, and would be extremely difficult to parallelize effectively. Most implicit methods, including those derived in this work, seek to make some simplifications to Eq. (3.24) which simplify the left-hand side and make the solution procedure more tractable. This is the focus of the following chapters.